Phase Transitions in Monolayers of PS−PEO Copolymer at the Air−Water Interface

M. C. Fauré and P. Bassereau*

Laboratoire Physico Chimie Curie, UMR 168 CNRS-Curie, Institut Curie, 11 rue Pierre et Marie Curie, 75231 Paris Cedex 05, France

L. T. Lee and A. Menelle

Laboratoire Léon Brillouin, CE-Saclay, 91191 Gif sur Yvette Cedex, France

C. Lheveder

Laboratoire de Physique Statistique de l'Ecole Normale Supérieure, 24 Rue Lhomond, 75231 Paris Cedex 05, France

Received January 20, 1999; Revised Manuscript Received August 23, 1999

ABSTRACT: The structures and phase transitions occurring during the compression of polystyrene−poly(ethylene oxide) (PS−PEO) diblock copolymer monolayers at the air−water interface have been studied by surface pressure isotherms, neutron reflectivity, and Brewster angle microscopy. At low coverage, the EO monomers adsorb at the air−water interface, but the PEO layer is not purely bidimensional. At high coverage, the EO−interface interaction becomes repulsive. A brush structure has been observed with differences between the long and the short PEO chains attributed to the difference in the accessible range of surface concentration. For the longest chain, the PEO concentration profiles exhibit a superposition of a depletion layer near the interface and discontinuous profile characteristics of a two-phase brush described by the "*n*-cluster" theory. For the shortest chains, the profiles are "pseudoparabolic". Finally, Brewster angle microscopy shows that, for the long chains, the transition between the adsorbed and the brush structures is first order.

1. Introduction

Amphiphilic diblock copolymers are a category of block copolymers, which have been widely studied in particular for their ability to form monolayers at the air/water interface. They are constituted of a hydrophobic block anchoring the chains at the interface and of a hydrophilic block, which is soluble in the water subphase. Copolymer monolayers can also form at the surface of other solvent−air interfaces such as that of selective solvent for one of the two blocks; the other block, being in a bad solvent situation, is acting as a buoy for the polymer chain at the solvent−air interface. Similarly to short surfactant molecules, compression isotherms of the Langmuir films of copolymers can be performed. But, contrary to the case of lipid or fatty acid monolayers where a large variety of structural phase transitions are observed during the compression, only two phase transitions have been measured in copolymer monolayers. Both concern the conformational changes of the polymer chains. The first is a continuous phase transition between a mushroom conformation at low surface density where the chains do not overlap and a brush conformation at higher density where the chains are stretched. This situation is observed when the monomers of the soluble block have no attraction for the interface as is the case for poly(dimethylsiloxane)−polystyrene (PDMS−PS) at the surface of ethyl benzoate[1] or dioctyl phthalate.[2] The second type of conformational phase transition was first predicted by Alexander[3] and later by Ligoure[4] for chains adsorbed at the interface; for long chains, a first-order transition is expected between an adsorbed conformation at low surface density and a brush conformation at high density. This should be observed when the soluble monomers have an attractive interaction with the interface, as is the case for poly(ethylene oxide) (PEO) at the free surface of water.[5−8] So far, mainly two PEO-containing diblock copolymers have been studied: poly(methyl methacrylate)−poly(ethylene oxide) (PMMA−PEO)[8−11] and the polystyrene−poly(ethylene oxide) (PS−PEO).[12−17] The nature of the transition has not yet been investigated for PMMA−PEO although a pseudo-plateau is present in the pressure isotherms.[8] For PS−PEO, a first-order type of the transition has been inferred from the existence of a plateau in the isotherms[12,13,17] for the long chains, but a coexistence of the two phases has not yet been proved experimentally. The self-consistent-field (SCF)[12] and single-chain mean-field (SCMF)[17] theories have been specifically applied to these PS−PEO copolymers, but these theories fail to describe long chain molecules; they predict the existence of an inflection point in the isotherms for short chains but not the plateau observed for the long chains.

From a more practical point of view, PEO and all its derivatives have a wide range of biotechnical and biomedical applications.[18] PEO is well-known for reducing the adsorption of soluble proteins on surfaces (see for example ref 19). Moreover, the PEO solutions in water have a unique behavior with respect to temperature and pressure[20,21] due to hydrogen bonding between the PEO monomers and the water molecules: the quality of the solvent decreases when the temperature or the pressure[22] increases. Moreover, even in a good solvent situation, PEO aggregates have been found to be present in aqueous solutions.[23] De Gennes proposed

* To whom correspondence should be addressed: E-mail patricia.bassereau@curie.fr.

10.1021/ma9900840 CCC: $18.00
Published on Web 11/24/1999

the first theoretical model for the water-soluble polymer solutions: the "*n*-cluster model".[24] In these solutions, the pairwise interactions of monomers are repulsive while interactions among a cluster of $n > 2$ monomers are attractive. This gives rise to a bulk demixing. The same kind of phase transition may also occur in surface-tethered chains. Above a critical grafting density, the concentration profiles of water-soluble polymer brushes are predicted to show a coexistence between two fully separated phases:[25,26] a dense phase in the vicinity of the surface and a dilute phase far from the surface. Similarly, the compression of a "one-phase" PEO brush is expected to produce the same type of phase transition[26,27] within the brush.

Consequently, copolymers of PEO constitute very interesting molecules because two different types of phase transition are expected to occur during the compression of their monolayer at the air/water interface. At moderate surface density, the coexistence of an adsorbed layer and a brush should be observed. At higher density, a phase transition within the brush should also take place. In this paper, we have studied the structure of asymmetric PS−PEO monolayers at the air−water interface. If the PS block is short compared to the PEO block, it could be expected that its role is limited at anchoring the PEO chain at the air−water interface and that it has no influence on the surface pressure isotherm or on the segment profile of the PEO chain normal to the interface. But, as the PS block is repulsive to the PEO block, this should modify the attractive nature of the interface for the PEO and therefore the expected concentration profile of the PEO chains. The balance between these opposite interactions will depend on the surface density of copolymer, on the length of the PS block, and also on the temperature. An additional transition may be observed between a liquid state of the PS block with attractive interactions between the chains and a glassy state if the temperature is lowered or if the PS chain is longer. We can imagine that the competition attraction−repulsion will induce a larger desorption of the PEO monomers from the interface than in the case of a pure PEO monolayer when the surface density is increased. The concentration profile of the PEO brush should also be affected. Nevertheless, in two extreme situations, the concentration profile should reflect the two opposite situations. At low density, the surface will be essentially attractive for the PEO as for a pure homopolymer, whereas at high density, it should be completely repulsive as soon as the interface will be fully covered by the PS and a depletion layer could be expected in the vicinity of the interface. In this paper, we have used a Langmuir trough, and a very wide range of surface density has been achieved from $\sigma^* = \pi R_G^2 \sigma \leq 1$ to $\sigma^* \approx 60$ (σ is the surface density in the monolayer and R_G is the radius of gyration of the soluble block), and we have been able to investigate the existence of these phase transitions. From the analysis of the isotherms, we could conclude about the thickness of the adsorbed layer in the low-density regime. The specific role of the PS anchors on this region of the isotherm has also been shown. In the high surface density regime, the structure of the monolayer has been determined from neutron reflectivity measurements. The concentration profiles have been compared to the existing models, and the possibility of a phase transition within the brush has been examined. Finally, with Brewster angle microscopy, for a long chain (700 PEO monomers), we present the first experimental evidence of the coexistence (in the plateau region) of a dilute phase with an adsorbed conformation and a brush phase with an extended conformation.

Table 1. Characteristics of the Copolymers[a]

copolymer $N_{PS}-N_{PEO}$	M_w (g mol^{-1})	$M_{w,PS}$ (g mol^{-1})	$M_{w,PEO}$ (g mol^{-1})	$M_{w,PEO}/M_w$	$f_{PEO} = N_{PEO}/N$	$I = M_w/M_n$
0−205	9000	0	9000	1	1	1.10
13−118	6500	1300	5200	0.800	0.901	1.10
13−220	11000	1300	9700	0.882	0.952	1.14
30−100	7300	3000	4300	0.591	0.769	1.10
30−200	11800	3000	8800	0.747	0.870	1.12
31−96 (D)	7700	3500	4200	0.546	0.756	1.10
31−179 (D)	11400	3500	7900	0.692	0.852	1.13
31−320 (D)	17600	3500	14100	0.801	0.912	1.14
31−700 (D)	34300	3500	30800	0.898	0.958	1.18
43−64	7300	4500	2800	0.386	0.598	1.09
43−150	11000	4500	6500	0.594	0.777	1.11
43−329	19000	4500	14500	0.763	0.884	1.13

[a] M_w is the total molecular weight of the copolymer, $M_{W,PS}$ and $M_{W,PEO}$ are the molecular weights of the PS and PEO blocks, respectively. $f_{PEO} = N_{PEO}/N$ is the asymmetry of the copolymer, N_{PEO} and N_{PS} are the number of PEO and PS monomers, respectively, and $N = N_{PS} + N_{PEO}$. I is the mass polydispersity of the copolymer.

2. Materials and Experimental Techniques

2.1. Materials. We have used asymmetric diblock copolymers synthesized by sequential anionic polymerization, by Y. Gallot, C. Sadron Institute, Strasbourg, France. The hydrophobic block consists of a polystyrene (PS) chain having between 13 and 43 monomers. The hydrophilic block is an OH-terminated poly(ethylene oxide) (PEO) chain. The number of EO monomers varies between 64 and 700. In the following, the PS−PEO copolymer chain will be denoted as $N_{PS}-N_{PEO}$ where N_{PS} is the number of PS monomers and N_{PEO} the number of PEO monomers. The copolymers used in this work have a small polydispersity, and their characteristics are listed in Table 1. The $31-N_{PEO}$ copolymers have a partially deuterated PS block (60% of the molecular weight).

2.2. Surface Pressure Measurements. The surface pressure isotherms were obtained with a Teflon Langmuir film balance (Lauda-FW 2). The maximum available surface is 927 cm^2 and can be varied continuously by moving a Teflon barrier. The surface pressure Π was measured continuously by means of a Langmuir balance. The experiments were performed at $T = 18$ °C in a clean room. The Langmuir film was obtained by depositing small drops (with a precision microsyringe) of the copolymer dissolved in chloroform at the air−water interface. The copolymer concentration in the chloroform solution was of the order of a few g/L. Before compression, the film was allowed to equilibrate for 15 min to ensure full evaporation of the solvent and also to allow a readjustment of the molecules. The compression rate was kept constant at 55 Å^2/(molecule min).

2.3. Neutron Reflectivity. Neutron reflectivity experiments were performed on the time-of-flight reflectometer DESIR in the ORPHEE reactor (Leon Brillouin Laboratory, Saclay, France). The copolymer solution in chloroform was spread on D_2O in a Teflon trough, which was completely closed to minimize the evaporation of the subphase and the contamination of the water surface. The trough was not equipped with a moving barrier for the compression of the monolayer. Therefore, the surface density was increased successively by dropwise addition of the copolymer solution to the water surface. Data acquisition began after 30 min. The stability of the layer was monitored by measuring the surface pressure before and after each reflectivity measurement. It did not vary significantly (less than 1 mN m^{-1} over 12 h). We have checked that the pressure isotherms are not changed when the compression is achieved by successive addition of the copoly-

mer solution. Moreover, for every experiment, we have also checked that the correspondence between the quantity of copolymer spread on the water/air interface and the surface pressure we measure is in good agreement with the surface pressure isotherm.

The surface pressure ranged from 10 to 34 mN m^{-1}. Three $31-N_{PEO}$ copolymers were studied. The scattering length densities of deuterated water, PEO, and partially deuterated PS (60%) are respectively $Nb_{D_2O} = 6.4 \times 10^{-6}$ Å^{-2}, $Nb_{PEO} = 0.45 \times 10^{-6}$ Å^{-2} (calculated with the PEO volume density $\rho = 1.13$ g cm^{-3}), and $Nb_{PS} = 4.0 \times 10^{-6}$ Å^{-2}.

The neutron beam passed through quartz windows to enter and exit the sample cell chamber. The measuring time per spectrum was approximately 10−12 h. The neutron wavelengths ranged from about 3 to 25 Å. The incident angle was 1.32°, and the angular resolution was 0.04°. The accessible range of the momentum transfer vector **q** ($q = (4\pi \sin \theta)/\lambda$) was limited to 0.09 Å^{-1}. The critical angle for total reflection was accessible. The total reflection plateau was then used to determine the normalization factor; the background intensity was determined from the intensity scattered just off the specular angle.

Reflectivities were calculated by approximating the model profiles by a series of thin homogeneous slabs (constant Nb) and calculating the reflectivity from the stack of layers using the Fresnel equations with a Debye−Waller factor to describe the effect of roughness at the air surface.[28] The procedure used to adjust the reflectivity data consists of choosing a profile shape and then determining the corresponding parameters for which the calculated reflectivity curve fitted the best the experimental data. The best-fit parameters were determined by the minimization of

$$\chi^2 = \frac{1}{M-p}\sum_i^M [\log R_i - \log R(q_i)]^2 \frac{R_i^2}{\epsilon_i^2}$$

where M is the number of experimental points, p the number of fitting parameters, R_i the calculated reflectivity for $q = q_i$, $R(q_i)$ the experimental reflectivity, and ϵ_i the experimental error.

After this χ^2 minimization procedure, an additional test has been used in order to discriminate between different good fits and to check the physical consistency of our results. For each experiment, we have compared the PEO equivalent thickness in the melt h_{exp} (also called "surface excess") determined from the molecular area A of the experiment, with the value h_{fit} deduced from the fitting procedure. h_{exp} (in angstrom units) can easily be deduced from the relation $h_{exp} = M_{PEO}/6.02 \times 0.1\rho_{PEO}A$, where M_{PEO} is the PEO molecular weight (in g mol^{-1} units) and $\rho_{PEO} = 1.13$ g cm^{-3}. h_{fit} is given by

$$h_{fit} = \int_0^\infty \Phi(z)\, dz \qquad (1)$$

where $\Phi(z)$ is the PEO chains volume fraction profile deduced from the fit and related to the scattering length density profile $Nb(z)$ by

$$\phi(z) = \frac{Nb(z) - Nb_{D_2O}}{Nb_{PEO} - Nb_{D_2O}} \qquad (2)$$

Both values h_{exp} and h_{fit} must be very close to accept the fit.

2.4. Brewster Angle Microscopy. The Brewster angle microscope used in this study was built by J. Meunier at the Ecole Normale Supérieure (Paris, France). A detailed description of this microscope is given in ref 29.

Brewster angle microscopy takes advantage of the properties of polarized light. At the Brewster angle (for water, the Brewster angle is equal to 53°) and for a Fresnel interface, the reflection coefficient of a p-polarized wave (e.g., with the electrical field in the incidence plane) is equal to zero. For a real interface (with a thickness, a roughness, and eventually an anisotropy), this coefficient is minimal at the Brewster angle, but it does not cancel.

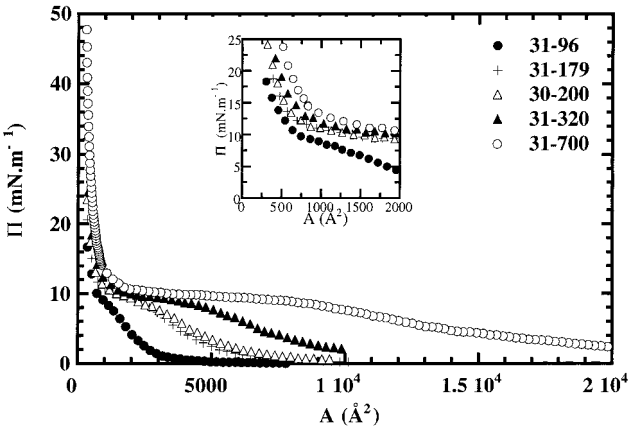

Figure 1. Effect of the PEO length on the surface pressure isotherms at $T = 18$ °C. Π is the surface pressure of the monolayer, and $A = \sigma^{-1}$ is the area per molecule. The PS size is fixed at 31 monomers (except one copolymer with 30 monomers), and the PEO length varies. The inset is an enlargement of the plot in the high-density region (low A).

If an amphiphilic molecule solution is spread on the surface, the optical index changes near the interface, so the Brewster condition is no more satisfied. If we assume that the layer has a thickness L and an index n, the reflection coefficient is given by

$$r_p(\theta) = r_s(\theta)\pi \frac{L}{\lambda} \frac{\sqrt{n_1^2 + n_2^2}}{n_1^2 - n_2^2} \frac{(n_2 - n_1^2)(n_2 - n_2^2)}{n^2} \qquad (3)$$

where θ is the incidence angle, $r_s(\theta)$ is the reflection coefficient of a s-polarized wave (e.g., for the electrical field perpendicular to the incidence plane) at the air/water interface, λ is the wavelength, n_1 is the refraction index of air, and n_2 is the refraction index of water.

For an amphiphilic molecules monolayer, the refraction index is generally larger than the refraction index of water and increases with molecules density (e.g., upon compression of the monolayer). If the monolayer is not homogeneous, the domains with different surface densities have different reflection coefficients. In particular, this is used to visualize the two different phases in a first-order phase transition region of a Langmuir film.

In our experiments, the copolymer solution was spread on the water surface at low surface density σ, in a Teflon trough isolated from the vibrations. After 15 min, the monolayer was compressed with a moving barrier, at a compression rate of 0.4 cm^2 min^{-1}. The surface pressure was measured continuously with a Wilhelmy plate. The barrier was stopped at different surface densities, and the corresponding images were recorded. The lateral resolution of the microscope is 1.5 μm. The experiments were carried out at $T = 19$ °C.

3. Results and Discussion

In Figure 1, we have plotted the experimental surface pressure−area (Π−A) isotherms corresponding to different PEO chain lengths, keeping the length of the PS block fixed at $N_{PS} = 31$. A is the area per molecule ($A = 1/\sigma$). The general shape of the isotherms is in agreement with previous experiments.[12] For each curve, three regions can be distinguished upon compression; they correspond to different chain conformations, which will be discussed further. We clearly observe two main differences compared to the nonattractive monomer−surface case studied by Kent et al. for example[1] with the monolayers of PS−PDMS at the ethyl benzoate/air

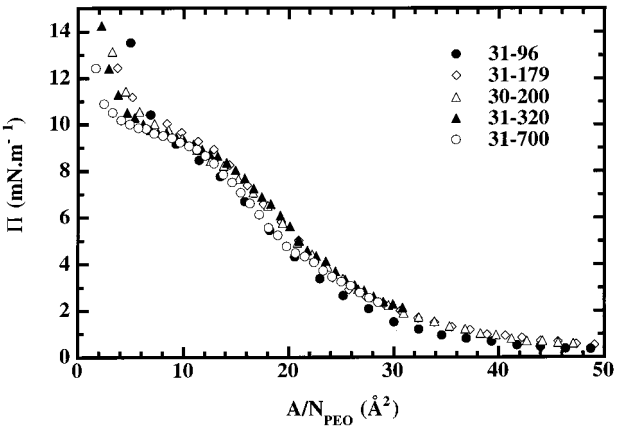

Figure 2. Surface pressure (Π) versus the renormalized surface per molecule (A/N_{PEO}). The copolymers and the corresponding symbols are the same as in the Figure 1.

interface. In their system, the soluble block in the liquid subphase (PS) has no surface activity, contrary to the case of the PEO in water. This difference is due to the amphiphilic nature of the EO monomers. First, a comparison of the variation of pressure with surface density σ in the low-density region (e.g., high area per molecule region) shows that the pressure increase in our system is much sharper that in the nonattractive case. In fact, when the monomers are attracted by the interface, their local density increases, resulting in a larger lateral monomer repulsion and hence a larger pressure. This has to be contrasted with the nonattractive interfaces where the chains are repelled from the surface (the "mushroom" regime). Second, as the monolayer is more compressed, we see a pseudoplateau which does not exist in the nonattractive case and which is a signature of the adsorption of the EO monomers at the air−water interface. Recently, we have used the single-chain mean-field (SCMF) theory to calculate the EO adsorption energy, which is found to be roughly -1.0 k_BT[17] where k_B is the Boltzmann constant and T the temperature.

Upon further compression, there is a very large increase in the pressure, which is also observed in Kent's system. In this regime of high density, a brush conformation is expected. No additional plateau or change in the slope of the isotherm is observed in the brush regime, as could be expected in the context of a second type of phase transition (the *n*-cluster model).

The effects of PEO and PS chain lengths on the shape of the pressure−area isotherms have been discussed in a previous paper.[17] The present paper is focused on the structures of the chains in the different phases.

3.1. Low Surface Density Region. The existence of an adsorbed layer at low surface coverage implies that in this region the pressure should exclusively be determined by the number of segments in the layer. Therefore, if the surface pressure is plotted versus the area per monomer, e.g., A/N_{PEO}, the rescaled isotherms should be independent of the numbers of monomers per chain. Figure 2 shows that for all A values higher than the onset of the plateau, the pressure isotherms can well be superimposed for $N_{PS} = 31$ and different PEO chain lengths. In all cases, this low-density region extends from $A/N_{PEO} = \infty$ to the lower limit $A/N_{PEO} \cong 12$ Å^2/monomer. We have divided this low-density region in two parts:

(a) For high A/N_{PEO} values larger than 44 Å^2, we are in the 2D dilute regime since, as is expected in this

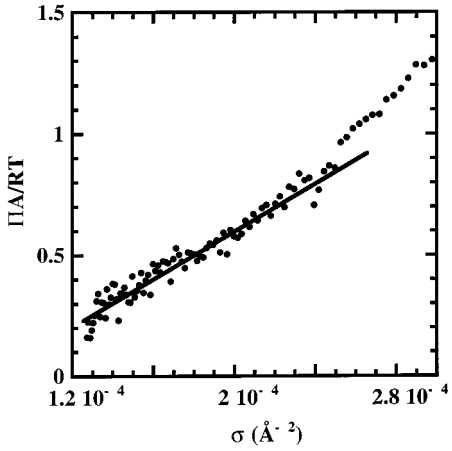

Figure 3. Evolution of the reduced quantity $\Pi A/RT$ with $1/A$ for the 31−96 copolymer in the dilute regime: Π is the surface pressure, A is the surface per molecule, R is the gas constant, and T is the temperature. The straight line corresponds to the linear regime, and the validity limit is $A = 4200$ Å^2/molecule.

Table 2. Fraction φ of the PEO Monomers Adsorbed at the Air−Water Interface in the Dilute Regime 3-1-a

copolymer	φ	copolymer	φ
13−118	0.87 ± 0.04	31−179	0.99 ± 0.02
13−220	0.98 ± 0.02	31−320	1.00 ± 0.06
30−100	1.06 ± 0.04	31−700	0.86 ± 0.04
30−200	1.00 ± 0.05	43−150	1.14 ± 0.06
31−96	0.96 ± 0.07	43−329	0.89 ± 0.04

regime (according to the Virial expansion[30]), the surface pressure Π varies linearly with $1/A^2 = \sigma^2$. Figure 3 represents $\Pi A/RT$ (R is the gas constant) as a function of $1/A$ for the copolymer 31−96, and we can clearly see the limit of the 2D dilute regime. A purely bidimensional monolayer has already been observed for pure PEO.[31] Note that a 2D ideal gas regime would be expected at very low density[32] but can never be reached experimentally for the polymer chains studied here. Indeed, we find that the crossover with the 2D ideal gas behavior will occur only at extremely large areas, at least 1 order of magnitude larger than the areas measured in our isothermal studies (for example, for $N_{PEO} \approx 100$, this crossover occurs at area per molecule of about 150 000 Å^2).[17]

By evolving a simple model based on the Flory−Huggins mean-field approach, we evaluate the fraction φ of the EO monomers adsorbed at the interface in this regime. Indeed, the linear relation between Π/N_{PEO}^2 and $1/A^2$ can be expressed as follows:[17]

$$\frac{\Pi}{N_{PEO}^{\ 2}} = k_BT\left[\frac{1}{2} - 2K\right]a_{EO}^{\ 2}\varphi^2\frac{1}{A^2} \qquad (4)$$

where $a_{EO} = 4$ Å is the ethylene oxide monomer size,[13,14,33] and $K \approx a_S^2 N_{PS}^{2/3}/a_{EO}^2 N_{PEO}$ (where $a_S = 5$ Å is the styrene monomer size) is a factor which ranges from 0.02 to 0.16 for the copolymers used in this study. From the slope of the experimental curves $\Pi/N_{PEO}^{\ 2} = f(1/A^2)$, and using eq 4, we can deduce φ the fraction of the EO monomers adsorbed at the interface. We find that φ is very high for each copolymer, always more than 85%. The φ values obtained for the copolymers used in this work are listed in Table 2.

(b) For higher surface densities, e.g., 44 Å$^2 \le A/N_{PEO} \le 12$ Å^2, the variation of the experimentally measured pressure is no longer linear with $1/A^2$ (Figure 3), clearly

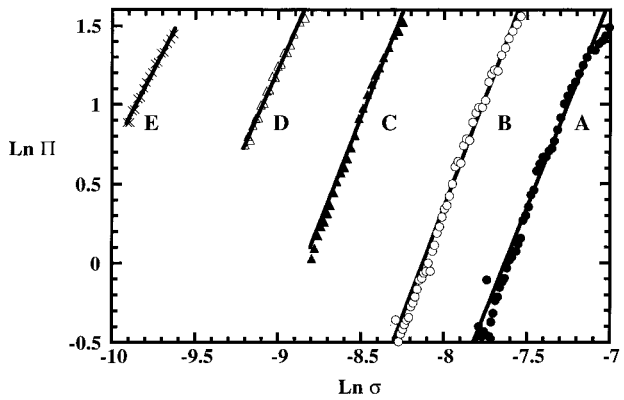

Figure 4. Determination of the exponent y of the eq 5 from the slopes of the ln Π versus ln 1/A plots in the low-density regime (3-1-b) for different copolymers: A, (43−64) $y = 2.65 \pm 0.02$; B, (31−96) $y = 2.78 \pm 0.03$; C, (31−179) $y = 2.66 \pm 0.03$; D, (31−320) $y = 2.40 \pm 0.02$; E, (31−700) $y = 2.06 \pm 0.02$. y is deduced from the best linear fits (solid lines).

showing the limit of the dilute regime. For these intermediate densities, the chains should interact more strongly than in the dilute regime. Two limiting cases can then be considered for their conformations: the polymer chains may interpenetrate at the interface, and a 2D semidilute regime could then be expected; another possibility corresponds to the desorption of part of the EO monomers from the air−water interface into the bulk to form a 3D semidilute layer. According to des Cloizeaux,[34] the surface pressure Π of a polymer monolayer in the semidilute regime is given by the following general expression:

$$\frac{\Pi}{T} \propto A^{-\nu d/(\nu d-1)} = A^{-y} \qquad (5)$$

where ν is the critical exponent of the excluded volume, d the space dimensionality, and $y = \nu d/(\nu d - 1)$. For chains in good solvent condition, which is the case for PEO in water at $T = 18$ °C, the exponent ν is theoretically predicted to be 0.75 for a 2D self-avoiding walk (SAW) and 0.6 for a 3D self-avoiding walk. Consequently, the theoretical exponent for the scaling of the surface pressure with the area per molecule is $y = 3$ for the 2D semidilute regime and $y = 2.25$ for the 3D semidilute regime. In Figure 4, we have plotted the variation of the surface pressure Π versus the inverse of the area per molecule 1/A on a double-logarithmic scale, for different copolymers, in the intermediate region between the dilute regime and the plateau. The slopes of these curves are directly equal to y. An exponent of 2.85 has been measured for long chains of pure PEO (more than 1000 monomers).[5] PEO molecules end-capped at both chain ends by short and hydrophobic segments (alkane groups C_{12} and C_{16}) also behave as 2D chains in a good solvent in a semidilute regime.[35] For PS−PEO copolymers with chain lengths similar to those discussed in this study, Bijsterbosch et al.[12] argued that the slopes appeared to be roughly consistent with $y = 3$. But, as these authors did not present fits of their experimental data, the exact value of the slope remains unclear. With our system, the value of y is below 2.85 for all chain lengths but larger than 2.25 excepted for the longest PEO chain (700 monomers). In this last case, the fit was done over a short interval of data due to the limited experimentally accessible area per molecule and probably close to the crossover with the plateau regime. Consequently, in this density range, the chain conformation is intermediate between a purely 2D entangled layer and a 3D interpenetrated layer. When the monolayer is compressed, the chains adopt a conformation with part of the segments still at the interface and some into the water subphase. As all segments are not adsorbed, the thickness of this monolayer should exceed the size of a monomer. Even for a pure PEO monolayer, a more accurate analysis using neutron reflectivity showed the presence of a diffuse layer under the interface,[36] indicating that 10% of the monomers are in the subphase. With the PS−PEO, the desorption of the monomers from the surface is certainly more important as shown from the surface pressure isotherms. The repulsive interactions between the PS and the PEO blocks can account for the difference in structure with pure PEO monolayer. In the case of PEO end-capped with alkane groups,[35] the hydrophobic ends are too small to have an influence at low surface coverage in the semidilute regime, so the isotherms obtained with a such polymer and a pure PEO (with the same chain length) are essentially identical in this region. Although the pressure isotherms deduced from SCMF predictions[17] are quasi superimposable with our experiments, this theoretical approach did not to predict a reduction of the volume fraction of adsorbed PEO monomers in this regime. No coupling between the PS and the PEO blocks other than having both the same surface coverage was introduced; in particular, the additional repulsive interaction between the two blocks was not taken into account.

A similar evolution of the conformations of adsorbed films of PEO−PMMA graft copolymers at the air/water interface was considered by Cardenas-Valera et al.[9] to interpret their data. Moreover, PM-IRRAS (polarization modulation infrared reflection−absorption spectroscopy) experiments performed on these monolayers showed that, on average, the mean axis of the molecules is not in the plane of the interface. In fact, the average tilt of the PEO chains with the interface plane is not constant when the monolayer is compressed[37] but increases with the surface density. This evolution confirms a partial desorption of some segments of the PEO chains increasing with the compression.

In principle, the extension of the layer in the third dimension could be measured experimentally using reflectivity techniques. Unfortunately, it is very difficult to measure the thickness of the layer and obtain a precise concentration profile due to the low density of monomers in the layer.

3.2. High Surface Density Region. At high coverage, the PEO block is expected to adopt a brushlike structure. The structure of highly stretched polymer brushes has been investigated theoretically with an analytical approach first by Alexander and de Gennes[3,38] and later by Milner, Witten, and Cates.[39,40] The former predicted, with scaling arguments, a step profile with a depletion layer close to the surface having a thickness independent of the surface density. The latter predicted a parabolic profile with a smooth tail.[41] This parabolic profile has been verified experimentally for long polymers densely grafted on a surface and with no attractive interaction between the monomers and the surface.[1,42−45] However, practical systems very often correspond to moderate molecular weights and grafting densities which can be better modeled by numerical approaches such as Monte Carlo,[46,47] molecular dynamics,[48−50] self-

consistent-field,[12,51−54] or single-chain mean-field theory[17,55−57] or by the renormalization group technique.[58] These theories are very useful for a correct description of experimental systems where a high grafting density may not be achieved[59−61] or for systems where the density may be continuously varied.[1,2,62] They predict the existence of a depletion layer with some variation in the position of the maximum volume fraction followed by a decrease and a smooth tail. For asymptotic limits in grafting density and molecular weights, the profiles are expected to be more and more parabolic as was shown for example by Kent et al.[1] For polymer chains exhibiting an attractive monomer−surface interaction, a pseudobrush profile is predicted[63,64] and observed[65,66] with a very high concentration of monomer at the surface.

It is interesting to compare the density profiles of the PS−PEO chains at the air−water interface with the existing theories and experimental data on polymer brushes and observe the consequence of the attractive PEO monomer−monomer interaction on the shape of the profile.

For this reason, neutron reflectivity experiments have been performed to determine the density profile of the PEO block for the high-compression regime, where a brush conformation is expected. Three copolymers have been studied: 31−96, 31−179, and 31−700 at different surface densities.

In our data analysis, the first layer of the model profile represents the PS layer that we describe as follows. To reduce the number of adjustable parameters, we assumed that in the dense region (after the plateau) the PS blocks spread on the water surface. The physical state of the PS chains has been discussed in a previous paper.[17] From the experimental results and the SCMF predictions, we concluded that the PS chains are liquid in bad solvent conditions and not glassy. Consequently, in a 2D liquid "collapse" state (bad solvent conditions and high-density regime), each PS chain occupies an area $A_{PS} = \pi(a_s N_{PS}^{1/2}/2)^2 = 630$ Å^2/molecule. Most of the neutron experiments were obtained at an area A below 630 Å^2/molecule. Consequently, we considered that we had a dense PS layer of thickness h_{PS} (in angstroms) given by the relation $h_{PS} = M_{PS}/6.02 \times 0.1\rho_{PS}A$, where M_{PS} is the PS molecular weight (in g mol^{-1} units), $\rho_{PS} = 1.05$ g cm^{-3} is the PS volume density, and A is expressed in Å^2/molecule. Consequently, h_{PS} ranges from 9 to 22 Å in the surface density range the experiments have been performed. Therefore, for the fitting procedure, the parameters h_{PS} and Nb_{PS} (PS scattering length density, in this case of pure polymer melt) were calculated, and only the roughness at the air−PS interface r_0 was fitted. When an experiment was performed at an area A higher than 630 Å^2/molecule, the three parameters Nb_{PS}, h_{PS}, and r_0 were fitted since the PS layer was no longer dense.

In order not to impose a priori a preferred profile for the PEO block, we tested different functional forms: the free profile, the parabolic profile, and the parabolic plus exponential profile. The details on these functions are given in the Appendix. In addition of these different shaped profiles, the possibility of a depletion layer near the surface has also been considered.

a. PS−PEO Copolymer 31−96. In Figure 5, we have plotted, for five different surface pressures, the reflectivity R from the monolayer divided by the calculated Fresnel reflectivity R_F for the pure solvent surface, e.g., deuterated water (D_2O). Such a curve will henceforth be referred to as "normalized reflectivity". The normalized reflectivity from the deuterated water surface is also plotted in the same figure. It was found in good agreement with the calculated Fresnel curve since $R/R_F = 1$. A 3 Å roughness was deduced from the analysis of the data for the D_2O. This representation shows clearly the decrease in reflectivity due to the PEO blocks and the oscillations in the curves from which the detailed concentration profile is determined.

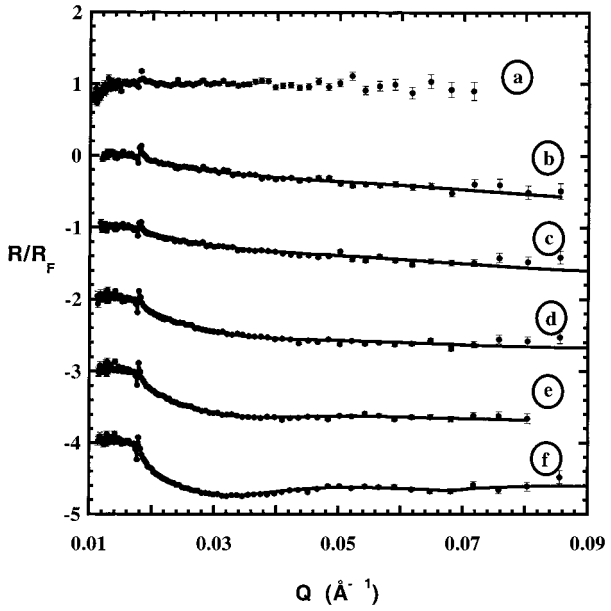

Figure 5. Normalized neutron reflectivity data for the pure D_2O interface (a) and for the 31−96 copolymer at different surface per molecule: 720 (b), 640 (c), 460 (d), 320 (e), and 250 Å^2/molecule (f). The dots correspond to the experimental data with their error bars and the full lines to the best fits with the respective concentration profiles plotted in Figure 6. For clarity reason, the plots have been arbitrarily downshifted by one unity.

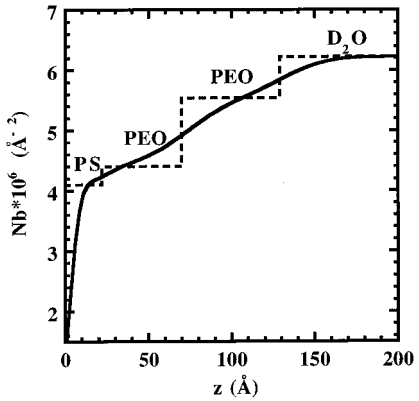

Figure 6. The three-layer scattering length density profile $Nb(z)$ (in continuous line) corresponding to the best fit of the reflectivity data of Figure 5f. The dashed line is a guide to the eyes to show the three layers of the same profile without roughness between the layers.

The continuous lines correspond to the calculated curves using a two-layer model profile. A typical complete profile of $Nb(z)$ obtained for a monolayer at $\Pi = 25$ mN m^{-1} (e.g., $A = 250$ Å^2 per molecule) is given in Figure 6. The experimental parameters (Π, A, and h_{exp}) and the h_{fit} and χ^2 values corresponding to the best fit are given in Table 3. We can see that the agreement between h_{exp} and h_{fit} is very good. The volume fraction

Table 3. Results of the Best Fits of the Neutron Reflectivity Data for the 31−96 and Comparison of the Surface Excess h_{Fit} Deduced from the Concentration Profiles of Figure 7 (Eq 1) and the Surfaces Excess Deduced from the Area per Molecule h_{exp}[a]

Π (mN m^{-1})	A (Å^2)	σ^*	h_{exp} (Å)	h_{fit} (Å)	χ^2
10	720 ± 30	3.2	16 ± 1	14 ± 1	1.68
11	640 ± 25	3.6	18 ± 1	15 ± 1	1.94
14	460 ± 20	5	26 ± 2	25 ± 1	2.00
18	320 ± 15	7.2	37 ± 3	34 ± 1	1.28
25	250 ± 15	9.2	47 ± 4	44 ± 1	1.93

[a] Π is the surface pressure, $A = 1/\sigma$ the molecular area (Å^2/molecule), σ^* the reduced surface density, and χ^2 the quality coefficient of the fit.

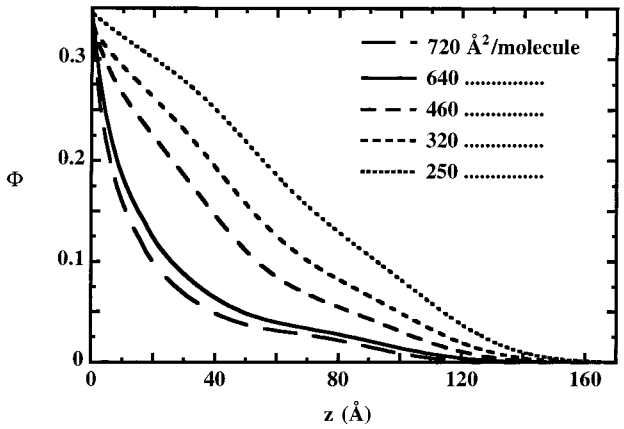

Figure 7. Density profiles Φ(z) of the PEO chains for the 31−96 copolymer at different surface per molecule corresponding to the best fits of the reflectivity data in Figure 5.

profiles of PEO chains $\phi(z)$ deduced from the best fits are shown in Figure 7.

The profiles, decreasing in concavity as the surface density increases, show clearly a densification of the monolayer. Moreover, as normally expected for brushes, the PEO chains are progressively stretched with increasing the surface density σ. No depletion layer is observed. A fit with a parabolic profile as predicted by the theory of Milner and co-workers is clearly inadequate ($\chi^2 > 6$). An exponential function could not be fitted to any data set either ($\chi^2 > 5$). In addition, we have checked that a simple scaling law profile $\phi(z) \propto z^{-4/3}$ could not fitted to the data, confirming that the PEO monolayer is not adsorbed at the interface.

b. PS−PEO Copolymer 31−179. A three-layer model profile for the PEO block is required to fit the experimental reflectivity curves. The measured and calculated normalized reflectivity curves are shown in Figure 8 for five different surface pressures. The experimental parameters, the h_{fit}, and χ^2 values deduced from the best fit are given in Table 4. As for the 31−96 copolymer, we observe a good agreement between the h_{fit} and h_{exp} values. The corresponding volume fraction profiles of PEO chains are given in Figure 9. At high surface pressures, 31−179 and 31−96 have very similar profiles. No depletion layer is observed in both cases. A stretching of the PEO chains with the surface density σ can be noticed. The data could be fitted as well, with equivalent χ^2 values, with a parabolic profile with an exponential tail (a pure parabola is inadequate). But, in this case, as the exponential contribution extends over half of the profile, the resulting profile is very far from a pure parabolic profile and very similar to the profile deduced with the three-layer model.

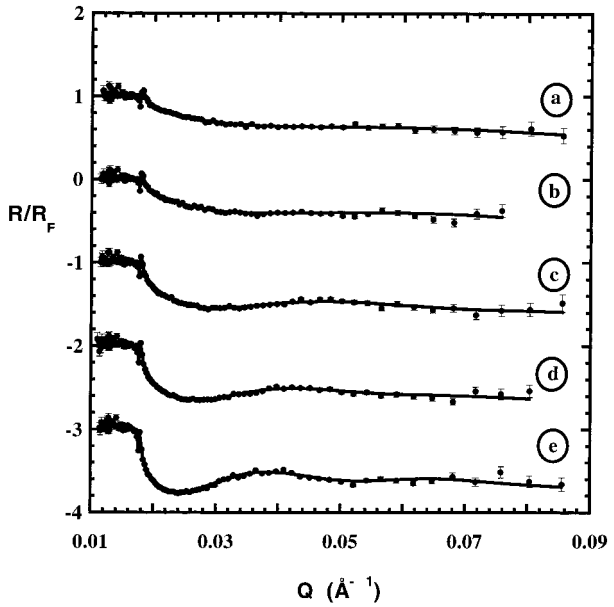

Figure 8. Normalized neutron reflectivity data for the 31−179 copolymer at different surface per molecule: 1130 (a), 790 (b), 530 (c), 360 (d), and 300 Å^2/molecule (e). Same remarks as in Figure 5.

Table 4. Results of the Best Fits of the Neutron Reflectivity Data for the 31−179 and Comparison of the Surface Excess h_{fit} Deduced from the Concentration Profiles in Figure 9 with Eq 1 and h_{Exp}; Notations Are Defined in Table 3

Π (mN m^{-1})	A (Å^2)	σ^*	h_{exp} (Å)	h_{fit} (Å)	χ^2
10.6	1130 ± 40	4.2	15 ± 1	16 ± 1	0.84
11.6	790 ± 30	6	22 ± 2	19 ± 1	1.36
15	530 ± 20	9	33 ± 4	28 ± 1	1.28
20	360 ± 15	13.3	48 ± 5	40 ± 1	1.26
28.5	300 ± 10	16	58 ± 5	52 ± 1	1.96

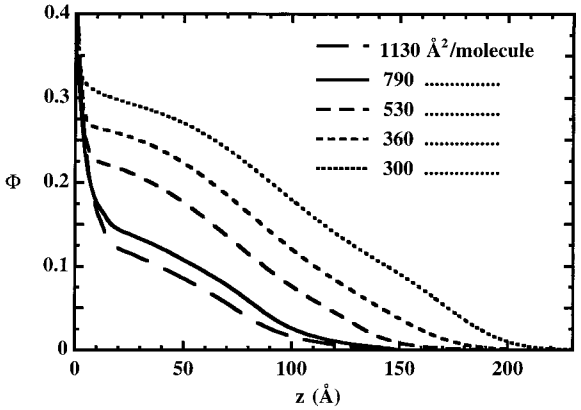

Figure 9. Density profiles Φ(z) of the PEO chains for the 31−179 copolymer at different surfaces per molecule corresponding to the best fits of the reflectivity data in Figure 8.

c. PS−PEO Copolymer 31−700. This copolymer is the longest of all the samples used in this work. No reasonable good fit was achieved with 3, 5, or 10 layers. Satisfactory results were obtained with the discretization of the PEO scattering length density profile in 20 layers. We start the fitting procedure with 20 layers of equal thickness and roughness. As the number of variable parameters is very high, we would expect that the result of the fit is not unique. However, the constraint parameter restricts the number of optimal fits. Moreover, we have checked that the profiles form deduced from the best fits (smaller χ^2 and reasonable

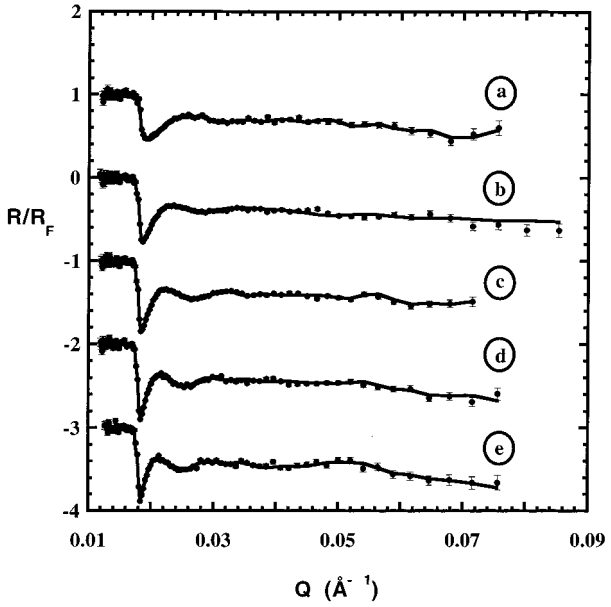

Figure 10. Normalized neutron reflectivity data for the 31−700 copolymer at different surface per molecule: 880 (a), 640 (b), 510 (c), 410 (d), and 370 Å²/molecule (e). Same remarks as in Figure 5.

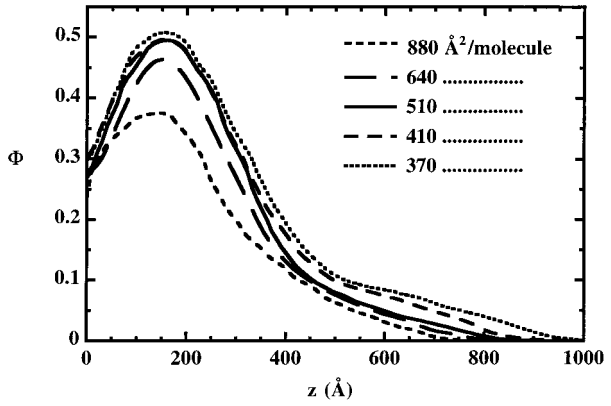

Figure 11. Density profiles Φ(*z*) of the PEO chains for the 31−700 copolymer at different surface per molecule and corresponding to the best fits of the reflectivity data in Figure 10.

Table 5. Results of the Best Fits of the Neutron Reflectivity Data for the 31−700 and Comparison of the Surface Excess h_{fit} Deduced from the Concentration Profiles in Figure 11 with Eq 1 and h_{exp}; Notations Are Defined in Table 3

Π (mN m^{-1})	A (Å^2)	σ*	h_{exp} (Å)	h_{fit} (Å	χ^2
14	880 ± 40	26.4	58 ± 5	128 ± 5	1.39
19	640 ± 30	36.3	80 ± 7	163 ± 8	1.44
24	510 ± 25	46	100 ± 8	183 ± 8	1.34
30	410 ± 20	57	124 ± 11	199 ± 10	1.60
34	370 ± 20	63	138 ± 13	215 ± 10	1.89

agreement between h_{fit} and h_{exp}) are independent of the initial values of the fitting parameters.

The h_{fit} and χ^2 values obtained for the optimized fits are listed in Table 5. The measured and calculated normalized reflectivity curves are shown in Figure 10. The corresponding volume fraction profiles of PEO chains are given in Figure 11. As for shorter chains, we observe that the PEO chains stretch when the surface density σ increases. But, the volume fraction profiles are very different from those obtained for the shorter chains. We clearly observe a depletion layer near the interface. Such a shape of profile with an important depletion layer has already been observed before for PEO homopolymer terminally bonded to polystyrene latex particles dispersed in water.[67,68] The thickness of the depletion layer is quite high, of the order of 140 Å, and obviously cannot be artifactually created by a poor estimation of the PS layer thickness. After the maximum, at a distance of about 140 Å from the interface, the profile first decreases steeply and then more slowly. This shape is very similar to that was predicted by the "*n*-cluster model".[25,26] It is discontinuous and exhibits two distinct regions: a "proximal" region near the surface where the PEO chains are closely packed and the density is high and a distal region with a low density which extends away from the surface.

Unlike the case of shorter chains, we observe a systematic discrepancy between h_{exp} and h_{fit} values: h_{fit} is 55−120% higher than h_{exp}, and no fit with a reasonable χ^2 corresponds to a good match of these values. Nevertheless, the general profile with a depletion and a bell-shape curve with an inflection point gives the best results whatever the initial parameters of the fit are. At the opposite with the shorter chains, a slope discontinuity in the distal region is required to obtain a good fit.

In contrast to what is claimed by Bijsterbosch et al.,[12] the best fits of our experimental curves with a parabolic plus exponential profile lead to nonacceptable χ^2 ($\chi^2 >$ 20) even if we include a depletion layer. The parabolic profile, even modified, therefore does not describe the concentration profiles of our system. We do not have any explanation for the differences between our observations and those reported in Bijsterbosch's experiments.

d. Discussion. The concentration profiles of the PS−PEO monolayers exhibit two main features, which differ depending on the length of the PEO chain. For the 31−700 copolymer, a depletion layer is present close to the interface whereas we did not measure it for the shorter chains. Moreover, the profiles of the 31−700 are clearly discontinuous, but they have a classical continuous shape for the 31−179 and 31−96 copolymers. We attribute this clear difference of the density profiles between the short chains and the long chain to the large difference in the reduced densities accessible in our experiments to the different copolymers. In fact, the surface density ranges in the "brush regime" are equivalent (from about 1000 Å²/molecule up to about 300 Å²/molecule) for the three copolymers, but they correspond to very different σ*: the ranges are [3−9], [4−16], and [26−63] for the 31−96, 31−179, and 31−700, respectively. The asymptotic limit should be reached at least for the 31−700 copolymer, and a "classical" parabolic profile could be expected barring any additional effect.

In the surface density range corresponding to the brush regime, the surface is totally covered by the PS block of the copolymer. As a consequence, the surface is no longer attractive to the EO monomers, as was the case in the dilute regime, but becomes repulsive to these monomers. The inversion of the nature of this interaction gives rise to the depletion layer we observe. This must be contrasted with the adsorbed layer existing at low surface densities.

In the 31−700 density profile, the thickness of the depletion layer (which is defined as the distance between the surface and the maximum in the profile) has been measured to be about 140 Å and to be independent of the surface density. This result is inconsistent with

the scaling theory of de Gennes.[69] This model predicts that the depletion layer should be independent of the molecular weight and of the order of $\sigma^{-1/2}$, e.g., from 17 to 34 Å in the density range accessible here.

More recently, Baranowski and Whitmore[54] used a numerical, self-consistent field theory (SCF), first developed by Whitmore and Noolandi,[52] to predict the structure of adsorbed diblock copolymers at a surface. In their model, they assumed that one block was tightly attached to the interface; the other block had no preferential interaction with the interface. The approach developed in refs 52 and 54 is valid for the whole range of the brush regime and not just for the asymptotic, highly stretched regime. They predict the existence of a depletion layer thicker than what was previously predicted by de Gennes. The position of the maximum is expected to be of the order of the radius of gyration R_G of the free polymer and only weakly dependent on the surface density (it varies as $\sigma^{-0.04}$). The same result was derived from a renormalization group approach.[58] These theories had been tested previously on another diblock copolymer[1] spread at a liquid interface, and a good agreement had also been observed.

In a first analysis, the thickness of the depletion layer of the 31−700 is in relatively good agreement with Whitmore et al.'s theory since $R_G = 0.215 M_W^{0.583\pm0.031}$ for an isolated PEO chain in water,[70] leading to $R_G = 90 \pm 28$ Å for the 700 monomers chain. However, the σ^* range reached in our experiments is very high compared to the typical densities these authors have considered in their papers, and the asymptotic limit described by the scaling theory should be reached. In principle, the SCF theory is not restricted to moderate surface density, but the scaling and the SCF approaches do not converge in the very dense regime as the latest predicts a very weak dependence with σ. In fact, the large depletion layer that we observe could be due to the combination of the attractive interactions between the PEO monomers, which become important as the EO concentration increases, and of the repulsive interaction between the PS at the interface and the EO monomers. Unfortunately, there is no model currently available taking properly into account the different interactions in our system and their dependence with the monomer density.

For the two short chains, the density range corresponds to the predictions of Whitmore et al.'s model, and a depletion layer should be present in the density profiles. If the size of the depletion layer is of the order of the free radius of gyration, we should expect to observe a maximum in the density profiles, at 28 Å for the 31−96 copolymer and at 40 Å for the 31−179. Indeed, the type of interaction of the EO with the surface should be independent of the PEO chain length, as long as all the EO monomers have desorbed from the surface. In fact, at the lowest surface densities of the 31−96 monolayer corresponding to σ^* of the order of 3 and to surface densities where the overlap of the PS chains is not fully achieved (720 and 640 Å^2/molecule), the desorption of the PEO from the interface is probably not complete. Actually, the profiles exhibit a concavity characteristic of an adsorbed layer. Similarly, for the two lowest densities of the 31−179 (see Figure 9), an adsorbed layer is present at the interface. Upon further compression, the profile shapes are analogous for the two copolymers, and no adsorbed layer is present any longer. The rise of the Φ profile very close to $z = 0$ observed for the highest densities in Figure 9 could result from the artificial cut in the density profile of the total layer corresponding to the thickness of the PS layer. The absence of a depletion layer in our fits of the highest densities data could be explained by the unfavorable contrast due to the partial deuteration of the PS block (60%), by the high roughness between the PS layer and the first PEO layer, and also by the limited resolution of the experimental setup. In Figure 12, we have plotted the length density profile $Nb(z)$, resulting in a good fit for the 31−96 copolymer at 25 mN/m. Contrary to the fit corresponding to Figure 6 (same copolymer in the same conditions), a depletion layer of thickness R_G (28 Å) has been added in the PEO profile; its thickness and its Nb value were fixed. The fitting procedure was then performed as usual. We see clearly that the contrast between the PS layer and the first PEO layer is low and that the roughness between the layers smoothes out the depletion layer. A better sensitivity could be probably achieved using a nondeuterated PS block, and the existence or absence of a depletion layer could be better elucidated.

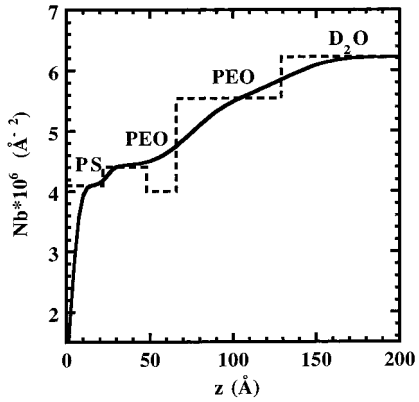

Figure 12. Effect of the roughness of the interface on the depletion layer. The length density profile $Nb(z)$ for the 31−96 copolymer at $\Pi = 25$ mN/m has been deduced from a good fit of the reflectivity data with conditions different from the Figure 6 (the plot symbols are identical to the Figure 6): the presence of a depletion layer has been imposed; its thickness has been fixed at $R_G = 28$ Å and $Nb = 4.4 \times 10^{-6}$ Å^{-2}. We clearly see that, with the low contrast between the PS layer and the depletion layer, a small roughness between them is sufficient to smooth out the depletion layer.

The short and long chains' density profiles differ also by the shape of the profiles beyond the position of the maximum. For the two short copolymers, besides the absence of a depletion layer due to our experimental limitations, the profiles are compatible with the predictions of Whitmore et al. on diblock copolymers[52,54] and observed on the PS−PDMS for example.[1] There is no evidence of a demixing along the brush chain for the highest densities accessible in our experiments. At the opposite end, the concentration profiles measured for the 31−700 are in good agreement with the existing theories on the "*n*-cluster model" in a brush layer and are a consequence of the attractive interactions between the EO units at high density. The corresponding reduced surface densities are in fact much higher for this copolymer than for the two shorter ones. Consequently, it is possible that, for the short copolymers, the surface densities achieved in this study are below σ_c at which the demixing occurs. In this case, the brushes would remain monophasic and have a classical profile, whereas for the long copolymer, the surface densities are above σ_c and two phases coexist in the brush. According to

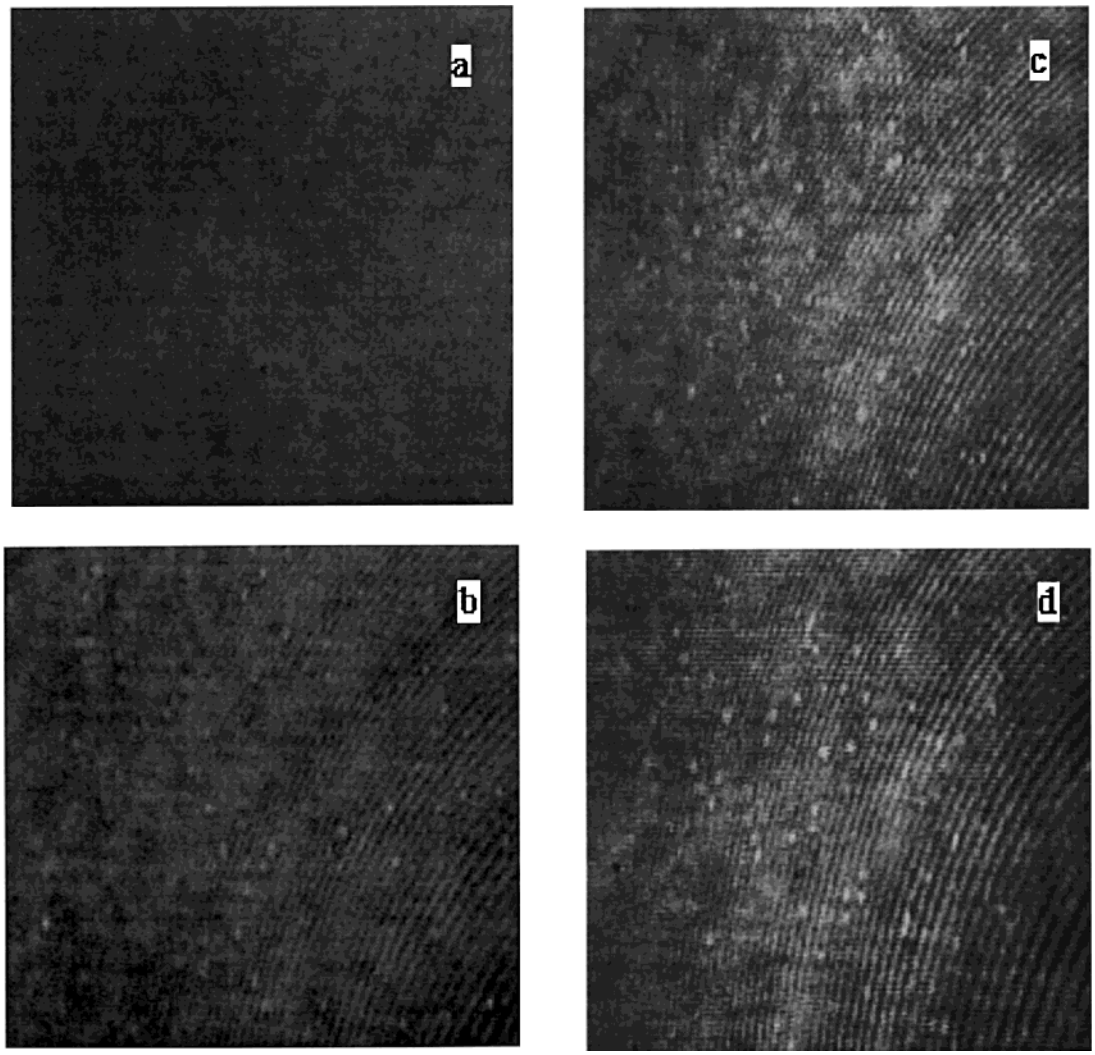

Figure 13. Brewster angle microscopy images of a 31−700 monolayer at different surface per molecule corresponding to the plateau region: 8000 (corresponding to the onset of the plateau) (a), 6000 (b), 4200 (c), and 1800 Å^2/molecule (d). The dimensions of the images are 270 × 270 μm^2.

Wagner et al., we would then expect an evolution of the respective proportion of the two regions, high and low density, with the compression. But, in fact, we observe that the boundary between the two regions is not displaced toward the tail region when the density in the brush is increased. The compression results in an increase of the concentration of the layer close to the surface. There are a few restrictive hypotheses in the SCF *n*-cluster theory. It supposes that the chains are disordered in the clusters, which may not be the case with PEO as its melting temperature is of the order of 60 °C. Moreover, the concentration profile has also to be invariant in the lateral direction: no patch must be present in the vicinity of the surface, and no lateral microphase separation must occur. The presence of peaks in preliminary grazing incidence X-ray diffraction spectra carried out at the LURE (Orsay, France) on these monolayers indicates that some ordered structures are present. The position of the peaks corresponds to a structure close to the PEO crystal structure. The artifactual origin of the peaks was ruled out, but further experiments are nevertheless required to investigate the evolution of size of the crystalline domains, their concentration, and possibly their structure with the surface density and the size of the PEO chains. The presence of ordered clusters in the monolayers might be responsible for the puzzling evolution of the concentration profile with the surface density.

Finally, no physical interpretation may be proposed for the almost constant value of the PEO volume fraction at $z = 0$ (the origin for the PEO layers). This value ranges between 0.3 and 0.4 independently of the chain length. This is most probably a consequence of our modeling of the PS layer and of the roughness of this interface.

3.3. The Transition Plateau. To our knowledge, there is no direct experimental observation of the coexistence of two phases in copolymer films at an interface.

Monolayers of three different copolymers (31−96, 31−320, and 31−700) have been studied with the Brewster angle microscope technique. Isotherms of these copolymers show a plateau that is horizontal only for the longest copolymer (31−700). Consequently, the transition "adsorbed layer to brush" is probably more and more of a first-order type as the PEO chain length increases. Unfortunately, due to the very low signal of the dilute phase, it was not possible to investigate a possible two-phase coexistence with neutron reflectivity.

Figure 13 shows images of a PS−PEO 31−700 monolayer at different surface densities. The field of view of the microscope remains uniform (Figure 13a) up to $A \approx$

7000 Å^2/molecule, which is slightly lower than the outset of the plateau on the isotherm (about 8000 Å^2/molecule). Then, small brilliant domains, with a diameter of about 10 μm, appear (Figure 13b). These bright regions correspond to dense domains dispersed in a lower density layer. The existence of these domains is clear evidence that the transition "adsorbed layer to brush" has a first-order nature. When the film is compressed in the plateau region, more and more brilliant domains appear (Figure 13c,d). The field of the microscope becomes lighter: a lot of domains with a diameter less than 10 μm and even less than the resolution of microscope ($\approx$1.5 μm) appear. The domains do not grow or coalesce. Moreover, if we stop the compression on the plateau (in the middle of the plateau for example), the brilliant points persist for at least 18 h, without any evolution: no relative motion and no coarsening were observed. When the compression reaches 1500 Å^2/molecule, which corresponds to the end of the plateau on the isotherm, the field of the microscope becomes uniformly bright. Since the size of the domains we have observed is very small, the resolution of the Brewster microscope used by Bijsterbosch et al.[12] using the same copolymer may have been too limited to observe these domains.

For shorter copolymers, 31−320 and 31−96, no domains were observed. The field of view of the microscope becomes uniformly lighter during the compression, and the transition appears to be continuous. However, if the size of the domains is below the 1.5 μm resolution of the microscope, they would not have been detectable. Nevertheless, as the PEO chain length decreases, the plateau of the isotherms becomes increasingly less horizontal, implying that the transition increasingly deviates from first order for chains shorter than 700 monomers.

Two different models have been proposed for describing this type of transition. Alexander[3] predicts a transition between a purely bidimensional adsorbed layer (pancake) and a brush at a surface density $\sigma_t \approx N^{-6/5}$, corresponding to the 3D overlap of the chains. On the other hand, Ligoure[4] predicts a transition between a self-similar adsorbed layer (SSAL) and a quasi-brush at a surface density $\sigma_t \approx \delta N^{-0.94}$ where $\delta k_B T$ is the adsorption energy of a monomer at the interface. Ligoure's model is in better agreement with our experimental results than the Alexander's on various aspects. First, we have shown that in the intermediate surface density region the thickness of the adsorbed layer phase probably exceeds the size of a monomer, as the monolayer is not purely bidimensional. Next, the transition (the outset of the plateau) occurs at a surface coverage A_t smaller than the overlapping value $A_{overlap} = \pi(a_{EO}N_{PEO}^{3/4}/2)^2$. For instance, for the 31−700 copolymer, $A_t \approx 8000$ Å$^2 \ll A_{overlap} \approx 230\,000$ Å^2 and $A_t \approx 1200$ Å$^2 \ll A_{overlap} \approx 12\,000$ Å^2 for the 31−96. Finally, if we use $\delta = 1$ (see beginning of section 3) for the value of the adsorption energy per EO monomer at the air−water interface as deduced from the SCMF theory,[17] and if we plot $\sigma_t = (A_t)^{-1}$ as a function of the number of EO monomers per chain N, we find that σ_t scales as $N^{-0.92\pm0.06}$ (Figure 14), which is in very good agreement with Ligoure's prediction. However, the structure of the brush postulated by Ligoure has never been observed in the high-density region. In his model, he assumes that the formation of the brush starts at the interface in the proximal part of the adsorbed layer profile, so that the brush develops outward from the surface; then, a self-similar adsorbed layer structure remains present but is gradually reduced and pushed outward.

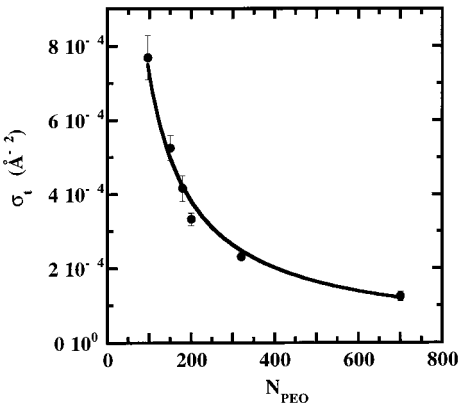

Figure 14. Variation of the surface density corresponding to the onset of the plateau σ_t with the number of PEO monomers in the copolymer N_{PEO}. The full line is the best fit with a power law $\sigma_t = AN^{\nu}$ with $A = 0.05$ and $\nu = -0.92 \pm 0.06$.

4. Conclusion

Spread monolayers of diblock copolymers of PS−PEO at the air−water interface were studied by surface pressure measurements, neutron reflectivity, and Brewster angle microscopy. One originality of the PS−PEO system is the possibility to tune the EO monomer−surface interaction just by changing the surface density of the monolayer. This requires a diblock copolymer with a high χ parameter and a strong affinity of the soluble block for the interface.

At low coverage, the interaction between the EO monomers and the interface is attractive, and the EO adsorb at the air−water interface. However, when the monolayer is compressed, the repulsive interactions between the PS and the PEO blocks promote the desorption of some EO monomers from the surface; the PEO chain conformation is not a purely bidimensional interpenetrated layer in the low-density region. The interaction between PS and PEO probably explains the difference observed between this copolymer monolayer and a pure PEO monolayer or PEO with very short anchors. Unfortunately, no reliable structural information could be obtained in the dilute region with neutron reflectivity, due to the low signal. Nevertheless, some preliminary X-ray reflectivity results suggest strongly that the thickness of the layer largely exceeds a monomer size. Moreover, PS−PEO copolymers are known to form micelles in solution.[71−73] These amphiphilic molecules may also self-assemble in two dimensions to form surface micelles.[74,75] The compression of surface micelles would lead, in the overlapping regime, to a layer thicker than a monolayer.[76,77] In this respect, atomic force microscopy or electron microscopy experiments on monolayers after transfer on a solid substrate would be very instructive.

Upon further compression, the PEO is pushed out of the surface layer into the water subphase to form a brush structure. At high coverage, the interface is completely covered with the PS blocks, and the interaction EO monomer−interface becomes repulsive, as supported by the presence of a depletion layer in the PEO chain volume fraction profiles deduced from the neutron reflectivity curves. The depletion layer has not been observed for the shortest chains when the desorption

of the EO monomers is fully achieved, but it may be smoothed out by the limited resolution of the setup, the roughness of the PS/PEO interface, and the partial deuteration of the PS block. Further experiments including PEO sizes intermediate between 200 and 700 monomers and a fully protonated PS block would certainly help to check the existence of the depletion layer for shorter chains and to measure the evolution of the profiles. For PEO chains shorter than 220 monomers, a precise prediction for the concentration profiles has been performed by Szleifer[17] with the SCMF (single-chain mean-field) theory, but the comparison is not adequate, as this model considers that the interaction PEO/surface is attractive for the whole density range.

For the long PEO chain and in the density range used in this study, the concentration profiles deduced from the fit of our neutron reflectivity data are compatible with the profile of a phase-separated brush, which is predicted by the *n*-cluster model. This transition results from the attractive interactions between the EO monomers at high concentration. This represents the first experimental evidence of a phase separation in a brush in the direction normal to the interface. The concentration profiles differ for the two short chains (31−96 and 31−179) and for the long one (31−700). This is probably due to the low reduced surface densities accessible to the short chains ($\sigma^* < 16$ in these experiments), which may correspond to densities below the phase transition. For these short copolymers, the profiles do not exhibit an inflection point, and they are similar to the "pseudo-parabolic" brush profiles of other copolymers.[1,52,54] To check the existence of a monophasic regime for the long chains and to characterize more precisely the transition toward the two-phase brushes, careful complementary experiments at densities intermediate between the density at the end of the plateau and $\sigma^* = 26$ for which the data have been collected are now necessary. Moreover, surface diffraction experiments are very promising for bringing new elements on the in-plane organization of the chains, on a possible lateral segregation reminiscent of a micellar structure, and on the presence of crystalline domains.

Finally, Brewster angle microscopy experiments allowed us to show for the first time that the transition between an adsorbed layer at low surface coverage and a brush structure at high surface coverage is a first-order transition for long chains as predicted by Alexander and Ligoure.[3,4]

Acknowledgment. We are grateful to Dr. M. Goldmann for his collaboration in the X-ray diffraction experiments on the line D41 at the LURE and for many helpful discussions. We want to thank also Drs. J. Daillant and P. Fontaine for their collaboration in the X-ray reflectivity measurements and Dr. C. Marzollin for the use of his profile fitting code. We are indebted to Pr. K. Shull for a critical reading of the manuscript.

Appendix. Functions Tested in the Fitting Procedures

Free Profile. The scattering length density profile $Nb(z)$ was discretized in n layers of constant Nb. To avoid artificial discontinuities due to the discretization, the number n was increased with the length of the PEO chains. The junction between the layers $i-1$ and i is not abrupt, and a roughness r_i between the layers was introduced. Then, the resulting expression $Nb_{i-1,i}(z)$ for the region of the profile intermediate between Nb_i and Nb_{i+1} is the following:

$$Nb_{i-1,i}(z) = Nb_{i-1} + \frac{Nb_i - Nb_{i-1}}{r_i\sqrt{\pi}} \times \int_{-\infty}^{z} \exp\left[-\frac{(u-h_i)^2}{r_i^2}\right] \mathrm{d}u$$

$$= Nb_{i-1} + \frac{Nb_i - Nb_{i-1}}{2}\left[1 + \mathrm{erf}\left(\frac{z-h_i}{r_i}\right)\right] \qquad (6)$$

with

$$\mathrm{erf}(z) = \frac{2}{\sqrt{\pi}}\int_0^z \mathrm{e}^{-t^2}\,\mathrm{d}t$$

The reflectivity data were then fitted by varying the different parameters. For each layer i ($i = 1, ..., n$), the three parameters $Nb_i(z)$, the thickness h_i, and the roughness r_i were fitted using the procedure already discussed in the Experimental Section. When the number of layers is higher than $n = 5$, a constraint parameter μ is introduced. A new function must be minimized instead of χ: $\chi'^2 = \chi^2 + \beta\mu$ where β is defined by $\beta = \sum_i (Nb_i - Nb_{i-1})^2$. The constraint parameter prevents the large variations in a profile, such as physically unrealistic serrated profiles. The choice of the value of μ is explained in ref 66 and in the references therein.

Parabolic Profile. We have also fitted the reflectivity data with a parabolic-type concentration profile. This corresponds to the following expression:

$$Nb(z) = Nb_{\mathrm{D_2O}} - (Nb_{\mathrm{D_2O}} - Nb_{\mathrm{PEO}})\Phi_0\left[1 - \left(\frac{z-h_{\mathrm{PS}}}{H}\right)^2\right], \quad h_{\mathrm{PS}} \le z \le h_{\mathrm{PS}} + H$$

$$Nb(z) = Nb_{\mathrm{D_2O}} \quad z \ge h_{\mathrm{PS}} + H \qquad (7)$$

where H is the PEO brush height and Φ_0 the average volume fraction of the PEO chains at $z = h_{\mathrm{PS}}$.

In this case, we have fitted $Nb_{\mathrm{D_2O}}$, Φ_0, H, and if necessary h_{PS}.

Parabolic Profile plus Exponential Tail. We have also tried to fit our data with a parabolic profile combined with an exponential tail, which allows for a smoother decrease in the profile at the extremity of the chains. This is given by

$$Nb(z) = Nb_1 = Nb_{\mathrm{D_2O}} - (Nb_{\mathrm{D_2O}} - Nb_{\mathrm{PEO}})\Phi_0\left[1 - \left(\frac{z - h_{\mathrm{PS}}}{H}\right)^2\right], \quad h_{\mathrm{PS}} \le z \le z_1$$

$$Nb(z) = Nb_2 = Nb_{\mathrm{D_2O}} - (Nb_{\mathrm{D_2O}} - Nb_{\mathrm{PEO}})\Phi_1 \times \exp\left[-\left(\frac{z - h_{\mathrm{PS}} - z_1}{z_2}\right)^2\right], \quad z_1 \le z \le z_2$$

$$Nb(z) = Nb_{\mathrm{D_2O}}, \quad z \le z_2 \qquad (8)$$

where Φ_1 is determined by the continuity condition

$Nb_1(z = z_1) = Nb_2(z = z_1)$. The fitted parameters are Nb_{D_2O}, Φ_0, H, Φ_1, z_1, z_2, and if necessary h_{PS}.

References and Notes

(1) Kent, M. S.; Lee, L. T.; Factor, B. J.; Rondelez, F.; Smith, G. *J. Chem. Phys.* **1995**, *103*, 2320.
(2) Kent, M. S.; Majewski, J.; Smith, G.; Lee, L. T.; Satija, S. K. *J. Chem. Phys.* **1998**, *108*, 5635.
(3) Alexander, S. *J. Phys. (Paris)* **1977**, *38*, 983.
(4) Ligoure, C. *J. Phys. II* **1993**, *3*, 1607.
(5) Kawaguchi, M.; Komatsu, S.; Matsuzumi, M.; Takahashi, A. *J. Colloid Interface Sci.* **1984**, *102*, 356.
(6) Kim, M. W.; Cao, B. H. *Europhys. Lett.* **1993**, *24*, 229.
(7) Cao, B. H.; Kim, M. W. *Faraday Discuss.* **1994**, *98*, 245.
(8) Gissing, S. K.; Richards, R. W.; Rochford, B. R. *Colloids Surf. A* **1994**, *86*, 171.
(9) Cardenas-Valera, A. E.; Bailey, A. I. *Colloids Surf. A* **1993**, *79*, 115.
(10) Richards, R. W.; Rochford, B. R.; Webster, J. R. P. W. *Polymer* **1997**, *38*, 1169.
(11) Peace, S. K.; Richards, R. W.; Taylor, M. R.; Webster, J. R. P. W.; Williams, N. *Macromolecules* **1998**, *31*, 1, 1261.
(12) Bijsterbosch, H. D.; de Haan, V.-O.; de Graaf, A. W.; Mellema, M.; Leermakers, F. A. M.; Cohen-Stuart, M. A.; van Well, A. A. *Langmuir* **1995**, *11*, 4467.
(13) Gonçalves da Silva, A. M.; Filipe, E. J. M.; d'Oliveira, J. M. R.; Martinho, J. M. G. *Langmuir* **1996**, *12*, 2, 6547.
(14) Prokop, R. M.; Hair, M. L.; Neumann, A. W. *Macromolecules* **1996**, *29*, 5902.
(15) Rother, G.; Findenegg, G. H. *Colloid Polym. Sci.* **1998**, *276*, 6, 496.
(16) Gonçalves da Silva, A. M.; Simoes Gamboa, A. L.; Martinho, J. M. G. *Langmuir* **1998**, *14*, 4, 5327.
(17) Fauré, M. C.; Bassereau, P.; Carignano, M.; Szleifer, I.; Gallot, Y.; Andelman, D. *Eur. Phys. J. B* **1998**, *3*, 365.
(18) Harris, J. M. In *Poly(ethylene glycol) Chemistry;* Plenum Press: New York, 1992.
(19) Andrade, J. D.; Hlady, V.; Jeon, S. I. In *Polyethylene oxide and protein resistance: principles, problems, and possibilities*; Glass, J. E., Ed.; Advances in Chemistry Series: American Chemical Society: Washington, DC, 1994.
(20) Matsuyama, A.; Tanaka, F. *Phys. Rev. Lett.* **1990**, *65*, 341.
(21) Bekinarov, S.; Bruinsma, R.; Pincus, P. A. *Phys. Rev. E* **1997**, *55*, 577.
(22) Cook, R. L.; King, H. E.; Pfeiffer, D. G. *Phys. Rev. Lett.* **1992**, *69*, 3072.
(23) Polik, W. F.; Burchard, W. *Macromolecules* **1983**, *16*, 6, 978.
(24) de Gennes, P. G. *C. R. Acad. Sci. Paris* **1991**, *313*, 1117.
(25) Wagner, M.; Brochard-Wyart, F.; Hervet, H.; de Gennes, P. G. *Colloid Polym. Sci.* **1993**, *271*, 1, 621.
(26) Sevick, E. M. *Macromolecules* **1998**, *31*, 1, 3361.
(27) Halperin, A. *Eur. Phys. J. B* **1998**, *3*, 359.
(28) Parrat, L. G. *Phys. Rev.* **1954**, *95*, 359.
(29) Hénon, S.; Meunier, J. *Rev. Sci. Instrum.* **1991**, *62*, 936.
(30) Huggins, M. *Makromol. Chem.* **1965**, *87*, 119.
(31) Kawaguchi, M.; Tohyama, M.; Takahashi, A. *Langmuir* **1988**, *4*, 411.
(32) Fleer, G. J.; Leermakers, F. A. M. *Curr. Opin. Colloidal Interfacial Sci.* **1997**, *2*, 308.
(33) Baekmark, T. R.; Elender, G.; Lasic, D.; Sackmann, E. *Langmuir* **1995**, *11*, 3975.
(34) des Cloizeaux, J. *J. Phys. (Paris)* **1975**, *36*, 281.
(35) Barentin, C.; Muller, P.; Joanny, J.-F. *Macromolecules* **1998**, *31*, 1, 2198.
(36) Lu, J. R.; Su, T. J.; Thomas, R. K.; Penfold, J.; Richards, R. W. *Polymer* **1996**, *37*, 109.
(37) Fauré, M. C.; Bassereau, P.; Desbat, B. *Eur. Phys. J. B*, in press.
(38) de Gennes, P. G. *Macromolecules* **1980**, *13*, 3, 1069.
(39) Milner, S. T.; Witten, T. A.; Cates, M. E. *Macromolecules* **1988**, *21*, 1, 2610.
(40) Milner, S. T.; Witten, T. A.; Cates, M. E. *Europhys. Lett.* **1988**, *5*, 413.
(41) Milner, S. T. *J. Chem. Soc., Faraday Trans.* **1990**, *86*, 1349.
(42) Field, J. B.; Toprakcioglu, C.; Ball, R. C.; Stanley, H. B.; Dai, L.; Barford, W.; Penfold, J.; Smith, G.; Hamilton, W. *Macromolecules* **1992**, *25*, 434.
(43) Auroy, P.; Mir, Y.; Auvray, L. *Phys. Rev. Lett.* **1992**, *69*, 93.
(44) Levicky, R.; Koneripalli, N.; Tirrell, M. *Macromolecules* **1998**, *31*, 1, 3731.
(45) Auroy, P.; Auvray, L.; Léger, L. *Phys. Rev. Lett.* **1991**, *66*, 719.
(46) Chakrabarti, A.; Toral, R. *Macromolecules* **1990**, *23*, 3, 2016.
(47) Lai, P. Y.; Binder, K. *J. Chem. Phys.* **1991**, *95*, 9288.
(48) Murat, M.; Grest, G. S. **1989**, *22*, 4054.
(49) Grest, G. S.; Murat, M. *Macromolecules* **1993**, *26*, 6, 3108.
(50) Grest, G. S. *Macromolecules* **1994**, *27*, 7, 418.
(51) Wijmans, C. M.; Scheutjens, J. M. H. M.; Zhulina, E. B. *Macromolecules* **1992**, *25*, 5, 2657.
(52) Whitmore, M. D.; Noolandi, J. *Macromolecules* **1990**, *23*, 3, 3321.
(53) Cosgrove, T. *J. Chem. Soc., Faraday Trans.* **1990**, *86*, 1323.
(54) Baranowski, R.; Whitmore, M. D. *J. Chem. Phys.* **1995**, *103*, 2343.
(55) Carignano, M. A.; Szleifer, I. *J. Chem. Phys.* **1994**, *100*, 3210.
(56) Szleifer, I.; Carignano, M. A. In *Advances in Chemical Physics;* Prigogine, I., Rice, S. A., Eds.; John Wiley & Sons: New York, 1996; p 165.
(57) Carignano, M. A.; Szleifer, I. *Macromolecules* **1995**, *28*, 8, 3250.
(58) Adamuti-Trache, M.; McMullen, W. E.; Douglas, J. F. *J. Chem. Phys.* **1996**, *105*, 4798.
(59) Satija, S. K.; Majkrzak, C. F.; Russell, T. P.; Sinha, S. K.; Sirota, E. B.; Hughes, G. J. *Macromolecules* **1990**, *23*, 3, 3860.
(60) Cosgrove, T.; Heath, T. G.; Phipps, J. S.; Richardson, R. M. *Macromolecules* **1991**, *24*, 4, 94.
(61) Perahia, D.; Wiesler, D. G.; Satija, S. K. K.; Fetters, L. J.; Sinha, S. K.; Milner, S. T. *Phys. Rev. Lett.* **1994**, *72*, 100.
(62) Kent, M. S.; Lee, L. T.; Farnoux, B.; Rondelez, F. *Macromolecules* **1992**, *25*, 6240.
(63) Aubouy, M.; Guiselin, O.; Raphaël, E. *Macromolecules* **1996**, *29*, 9, 7261.
(64) Aubouy, M. *Phys. Rev. E* **1997**, *56*, 3370.
(65) Guiselin, O. *Europhys. Lett.* **1992**, *17*, 225.
(66) Marzolin, C. Thèse de doctorat, Université de Paris VI, France, 1995.
(67) Cosgrove, T.; Crowley, T. L.; Vincent, B. In *An experimental study of polymer conformations at the solid/solution interface;* Ottewill, R., Rochester, C., Smith, A., Eds.; Academic Press: London, 1983; p 287.
(68) Cosgrove, T.; Heath, T. G.; Ryan, K.; Van Lent, B. *Polym. Commun.* **1987**, *28*, 64.
(69) de Gennes, P. G. *Macromolecules* **1981**, *14*, 4, 1637.
(70) Devanand, K.; Selser, J. C. *Macromolecules* **1991**, *24*, 4, 5943.
(71) Caldérara, F.; Hruska, Z.; Hurtrez, G.; Lerch, J.-P.; Nugay, T.; Riess, G. *Macromolecules* **1994**, *27*, 7, 1210.
(72) Xu, R.; Winnik, M. A.; Riess, G.; Chu, B.; Croucher, M. D. *Macromolecules* **1992**, *25*, 5, 644.
(73) Cogan, K. A.; Gast, A.; Capel, M. *Macromolecules* **1991**, *24*, 4, 6512.
(74) Zhulina, E. B.; Singh, S.; Balazs, A. C. *Macromolecules* **1996**, *29*, 9, 6338.
(75) Clarke, C. J.; Zhang, L.; Zhu, J.; Yu, K.; Lennox, R. B.; Eisenberg, A. *Macromol. Symp.* **1997**, *118*, 647.
(76) Daoud, M.; Cotton, J. P. *J. Phys. (Paris)* **1982**, *43*, 531.
(77) Zhulina, E. B.; Vilgis, T. A. *Macromolecules* **1995**, *28*, 8, 1008.

MA9900840